

Huijong Han^{a,b} and Petri
Kursula^{a,b,c,d,*}^aFaculty of Biochemistry and Molecular
Medicine and Biocenter Oulu, University of
Oulu, PO Box 3000, FIN-90014 Oulu, Finland,^bCentre for Structural Systems Biology,
Helmholtz Centre for Infection Research
(CSSB-HZI), German Electron Synchrotron
(DESY), Hamburg, Germany, ^cDepartment of
Chemistry, University of Hamburg, Hamburg,
Germany, and ^dDepartment of Biomedicine,
University of Bergen, Bergen, NorwayCorrespondence e-mail:
petri.kursula@biomed.uib.noReceived 3 July 2014
Accepted 9 September 2014

Expression, purification, crystallization and preliminary X-ray crystallographic analysis of the extracellular olfactomedin domain of gliomedin

Gliomedin (GLDN) is one of the essential proteins in the development of the nodes of Ranvier in the vertebrate peripheral nervous system. An olfactomedin (OLF) domain is located at the GLDN extracellular C-terminus and is involved in the accumulation of neuronal plasma membrane voltage-gated sodium channels in the nodes by interacting with neurofascin and NrCAM. No structures of OLF domains have previously been reported. Here, the crystallization of the rat GLDN OLF domain, which was expressed in an insect-cell system, is reported. The crystal diffracted to 1.55 Å resolution and belonged to space group $P2_1$, with unit-cell parameters $a = 37.5$, $b = 141.7$, $c = 46.0$ Å, $\beta = 110.6^\circ$, and had two molecules in the asymmetric unit.

1. Introduction

Myelin is a highly insulating, multilayered proteolipid membrane that is wrapped around selected neuronal axons in the nervous system. The nodes of Ranvier are the gaps formed between myelin sheath segments along the axons containing a high density of voltage-gated sodium channels (VGSCs) on the axonal membrane. The accumulation of VGSCs at the nodes leads to rapid saltatory nerve impulse conduction along myelinated axons (Waxman & Ritchie, 1993).

Gliomedin has been reported to be one of the major players in the development of the nodes of Ranvier on myelinated axons. It is a glial ligand for neurofascin and NrCAM, two axonal immunoglobulin cell-adhesion molecules associated with VGSCs at the nodes of Ranvier. Gliomedin is expressed by myelinating Schwann cells in the peripheral nervous system and accumulates at the edges of each myelin segment during development (Eshed *et al.*, 2005, 2007; Feinberg *et al.*, 2010).

Gliomedin (GLDN) is an *N*-glycosylated trimeric molecule consisting of a transmembrane domain, two collagenous domains and an olfactomedin (OLF) domain (Maertens *et al.*, 2007), and the extracellular domain can be released by proteolytic cleavage (Eshed *et al.*, 2007). It has been reported that the OLF domain is responsible for interaction with the FnIII domains of neurofascin and NrCAM (Labasque *et al.*, 2011) and that these interactions are important for inducing the formation of the nodes of Ranvier (Eshed *et al.*, 2005). The disruption of such interactions may be responsible for several human neuropathies such as Guillain-Barré syndrome and chronic inflammatory demyelinating polyneuropathy (Lonigro & Devaux, 2009; Devaux, 2012).

To date, at least 13 OLF-domain-containing proteins are known and they play important roles in various processes such as neurogenesis, neural crest formation, cell–cell adhesion and cell-cycle regulation. However, the biological functions of these proteins at the molecular level remain unclear for the most part (Tomarev & Nakaya, 2009; Anholt, 2014). Here, we have taken the first steps towards structure determination of GLDN. The extracellular OLF domain was expressed recombinantly, purified and crystallized. The results will eventually shed light on the neuroglial interactions in the PNS (peripheral nervous system), as well as provide a structural basis to study other proteins with OLF domains.

© 2014 International Union of Crystallography
All rights reserved

Table 1

GLDN OLF production information.

In the primers, the region corresponding to the TEV cleavage site (ENLYFQ/G)-GLDN is shown in capital letters. In the protein sequence, the GLDN sequence after TEV protease cleavage is underlined.

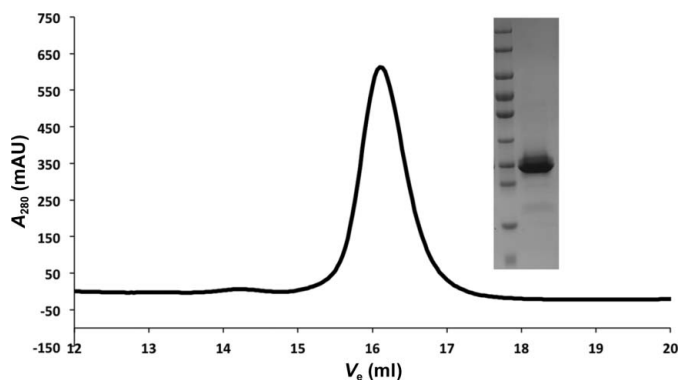
Source organism	<i>Rattus norvegicus</i>
Forward primer	5'-cag gga ccc ggt GAG AAT CTT TAT TTT CAG GGC-3'
Reverse primer	5'-cga gga gaa gcc cgg tta TGA CGA AAA GTG CA-3'
Expression vector	pFastBacNKI-His-3C-LIC
Expression host	<i>Spodoptera frugiperda</i> (<i>Sf21</i>)
Complete amino-acid sequence of the construct produced	MAHHHHHSAALEVLFQGPGENLYFQQPNSFTNQCPGETCV- IPNDLTVGRADEK VNERHSPQTEPMITSIGNPAQVLKVK- ETFGTWLRESANRSDRIWVTEHFSGIMVKEFEDLPALLN- SSFTLLHLPYFHGGHAYVNNLSLYHKGGSNITIVRFEFG- KETPQTLKLEDALYFDRKYL FANSKYFNIAVDEKGLWII- YASSVDGSSILVAQLDERTFSLRHINTTYPKSKAGNAFI- AQGILYVTDKTRVTFADLLRQKINANFGLRMSQSVL- AMLSYNMRDQHLYSWEDGHLMLYPVHFSS

2. Materials and methods

2.1. Cloning, baculovirus preparation and recombinant protein production

The cloning was started from a plasmid prepared for *Escherichia coli* expression tests encoding the rat GLDN OLF domain (residues 260–543; accession No. AAP22419) in the pHMGWA vector containing an N-terminal *Tobacco etch virus* (TEV) protease cleavage site. The coding insert was amplified by PCR using the primers shown in Table 1. *DpnI* was added to the PCR products to digest the template DNA. The pFastBacNKI-His-3C-LIC vector (Luna-Vargas *et al.*, 2011) was amplified in DH5 α *E. coli* cells, extracted using the QIAprep Spin Miniprep Kit (Qiagen) and then treated with *KpnI* for linearization. The amplified insert and the *KpnI*-treated vector were purified by agarose gel extraction using the QIAquick Gel Extraction Kit (Qiagen). The purified insert and vector were treated separately with T4 polymerase (New England Biolabs) at room temperature for 20 min and the reaction was stopped by the addition of 25 mM EDTA followed by inactivation of the T4 polymerase at 348 K for 20 min. The annealing reaction was performed by mixing the same molar amount of vector and insert. The reaction mixture was incubated at 338 K for 10 min, cooled to 295 K and used for transformation into NEB5DH10EMBacY cells, which were then used for bacmid preparation.

Sf21 insect cells were transfected with the GLDN OLF bacmid using the FuGene 6 transfection reagent (Promega) and the virus was


Figure 1

Elution profile of purification of rat GLDN OLF recorded on an ÄKTApurifier FPLC system (GE Healthcare) at 280 nm wavelength. The SDS-PAGE of the purified protein, corresponding to the elution peak, is shown as an inset.

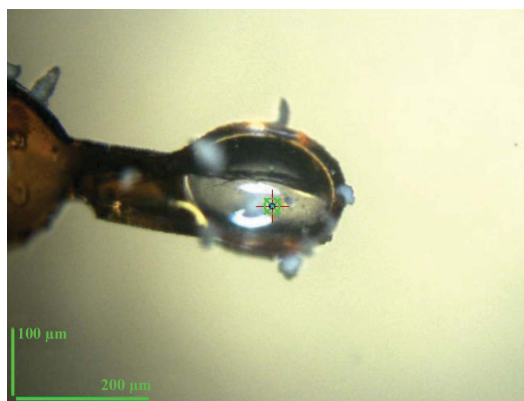
Table 2

Crystallization conditions.

Method	Sitting-drop vapour diffusion
Plate type	Swissci MRC 2 96-well plates
Temperature (K)	293
Protein concentration (mg ml ⁻¹)	10
Buffer composition of protein solution	50 mM Tris-HCl pH 7.5, 400 mM NaCl, 1 mM DTT
Composition of reservoir solution	100 mM sodium citrate pH 5.5, 20% PEG 3000
Volume and ratio of drop	0.3 μ l protein + 0.3 μ l reservoir
Volume of reservoir (μ l)	50

harvested after 72 h of infection (Bieniossek *et al.*, 2008). The recombinant primary virus was amplified to a high-titre viral stock. For protein expression in the insect-cell culture, 7.5 μ l high-titre virus was used per 25 ml 0.75×10^6 cells ml⁻¹. The infected cells were incubated at 300 K for 72 h before harvesting by centrifugation at 150g for 15 min. The cell pellets were resuspended in lysis buffer [50 mM Tris-HCl pH 7.5, 400 mM NaCl, 2 mM β -mercaptoethanol (BME) and cOmplete Mini protease-inhibitor cocktail (Roche)] and lysed by sonication. The soluble fraction was separated from cell debris by centrifugation at 14 500g for 30 min at 277 K.

The supernatant was loaded onto an Ni-NTA gravity-flow column pre-equilibrated with lysis buffer containing 20 mM imidazole. Unbound proteins were washed out with ten column volumes of the same buffer and the bound proteins were eluted using lysis buffer supplemented with 500 mM imidazole. After buffer exchange of the eluate back to lysis buffer using a PD-10 column (GE Healthcare), the protein concentration was measured and a 1:10(*w:w*) ratio of His-tagged TEV protease (van den Berg *et al.*, 2006) was added to cleave the N-terminal His tag from the target protein. The cleavage reaction was carried out at 277 K overnight. To remove the cleaved His tag, the reaction mixture was then poured onto an Ni-NTA gravity-flow column and the flowthrough and five column volumes of washing fractions were collected and concentrated. The final step of purification was performed by size-exclusion chromatography using a Superdex 200 10/300 GL column (GE Healthcare), eluting with the lysis buffer (Fig. 1). The fractions corresponding to the main peak were pooled and concentrated to 10 mg ml⁻¹ by centrifugal ultrafiltration using Vivaspinn devices with a 10 kDa molecular-weight cutoff (Sartorius). The identity of the purified protein was confirmed by mass spectrometry (data not shown).


Figure 2

A mounted cryocooled crystal of GLDN OLF formed using 20% PEG 3000, 0.1 M sodium citrate pH 5.5. The length of the used crystal was greater than 200 μ m with 70 μ m width.

2.2. Crystallization

Crystallization screening of purified concentrated GLDN OLF was performed at 293 K by sitting-drop vapour diffusion on an MRC 96-well plate using the JCSG+ screen from Molecular Dimensions and the PEG/Ion and Crystal Screen Lite screens from Hampton Research. Crystallization droplets were prepared by mixing 0.3 μ l protein solution and 0.3 μ l reservoir solution and were equilibrated against 50 μ l reservoir solution. Initial crystals were formed in the condition 0.1 M sodium citrate pH 5.5, 20% PEG 3000 after overnight incubation; they had a very thin plate shape and were extremely fragile. These crystals disappeared after a few days, but thicker and larger crystals were found three months later. A crystal was used for diffraction data collection without further optimization. The detailed crystallization protocol is given in Table 2.

2.3. Data collection and processing

X-ray diffraction data were collected using synchrotron radiation on beamline ID23-2 (Flot *et al.*, 2010) at the ESRF, Grenoble, France (Table 3). The crystals were first soaked in reservoir solution supplemented with 20% PEG 200 as a cryoprotectant and were then flash-cooled in liquid nitrogen. Diffraction data were collected to 1.55 Å resolution and the data were processed using XDS (Kabsch, 2010). Data-processing statistics and further details of data collection are given in Table 3.

3. Results and discussion

After significant effort, failure to overexpress GLDN OLF in *E. coli* with various expression vectors (unpublished data) made us move on to an insect-cell expression system. Consequently, GLDN OLF was successfully overexpressed in Sf21 insect cells and purified as a soluble monodisperse protein. Small-angle X-ray scattering experi-

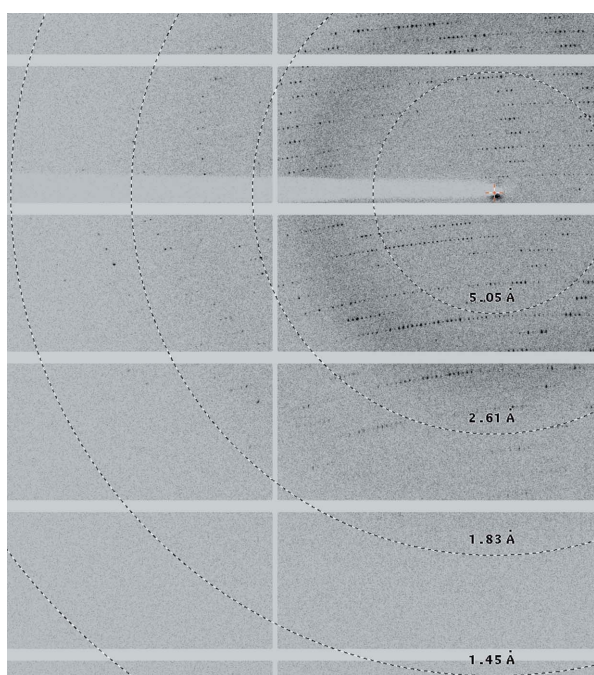


Figure 3 Diffraction pattern from the crystal used for data collection. Spots can be observed to a high-resolution limit of approximately 1.6 Å.

Table 3

Data-collection and processing statistics for GLDN OLF.

Values in parentheses are for the outer shell.

Diffraction source	ID23-2, ESRF
Wavelength (Å)	0.873
Temperature (K)	100
Detector	PILATUS 2M
Crystal-to-detector distance (mm)	169.68
Rotation range per image (°)	0.1
Total rotation range (°)	200
Exposure time per image (s)	0.05
Space group	$P2_1$
a, b, c (Å)	37.5, 141.7, 46.0
α, β, γ (°)	90, 110.6, 90
Resolution range (Å)	20–1.55 (1.60–1.55)
Total No. of reflections	230983
No. of unique reflections	64294
Completeness (%)	98.9 (98.2)
Multiplicity	3.6 (3.5)
$\langle I/\sigma(I) \rangle$	9.5 (2.0)
R_{meas} (%)	10.5 (78.6)
Overall B factor from Wilson plot (Å ²)	21.3

ments showed that GLDN OLF exists as a monomer in solution (data not shown).

Crystallization screening was performed with commercially available screens. The thin initial crystals were also picked and tested using synchrotron radiation; however, diffraction was very poor. Better-quality crystals were formed and grown to a size of >200 μ m (Fig. 2) after three months of incubation and these were used for data collection (Table 3; Fig. 3). The GLDN OLF crystals belonged to space group $P2_1$, and the calculated Matthews coefficient suggests one (V_M of 3.53 Å³ Da⁻¹, 65.2% solvent content) or two (V_M of 1.77 Å³ Da⁻¹, 30.4% solvent content; Matthews, 1968) monomers per asymmetric unit. A self-rotation function calculated from the diffraction data indicated the presence of a twofold noncrystallographic symmetry axis at $\theta = 69.3^\circ$, $\varphi = 0^\circ$, clearly showing the presence of two monomers in the asymmetric unit.

To date, no olfactomedin domain structure has been reported and the protein of known structure with the highest sequence identity to our construct displays only 10% identity. Hence, structure determination by molecular replacement is likely to be impossible at present. Currently, experimental phasing trials using different methods and derivatives are under way.

The crystal structure of GLDN OLF will be the very first structure of any olfactomedin domain. We expect that the GLDN OLF structure will be useful in obtaining insights into the detailed molecular function of gliomedin in the development of the nodes of Ranvier in the vertebrate peripheral nervous system. It can also be used to study epitopes recognized by antibodies in neurological autoimmune diseases.

This work has been supported by grants from the Academy of Finland, the Sigrid Jusélius Foundation and the Research and Science Foundation of the City of Hamburg. The research leading to these results has received funding from the European Community's Seventh Framework Programme (FP7/2007–2013) under BioStruct-X (grant agreement No. 283570).

References

- Anholt, R. R. H. (2014). *Front. Cell Dev. Biol.* **2**, 6.
- Berg, S. van den, Löfdahl, P. A., Härd, T. & Berglund, H. (2006). *J. Biotechnol.* **121**, 291–298.
- Bieniossek, C., Richmond, T. J. & Berger, I. (2008). *Curr. Protoc. Protein Sci.*, Unit 5.20. doi:10.1002/0471140864.ps0520s51.
- Devaux, J. J. (2012). *Am. J. Pathol.* **181**, 1402–1413.

- Eshed, Y., Feinberg, K., Carey, D. J. & Peles, E. (2007). *J. Cell Biol.* **177**, 551–562.
- Eshed, Y., Feinberg, K., Poliak, S., Sabanay, H., Sarig-Nadir, O., Spiegel, I., Bermingham, J. R. Jr & Peles, E. (2005). *Neuron*, **47**, 215–229.
- Feinberg, K., Eshed-Eisenbach, Y., Frechter, S., Amor, V., Salomon, D., Sabanay, H., Dupree, J. L., Grumet, M., Brophy, P. J., Shrager, P. & Peles, E. (2010). *Neuron*, **65**, 490–502.
- Flot, D., Mairs, T., Giraud, T., Guijarro, M., Lesourd, M., Rey, V., van Brussel, D., Morawe, C., Borel, C., Hignette, O., Chavanne, J., Nurizzo, D., McSweeney, S. & Mitchell, E. (2010). *J. Synchrotron Rad.* **17**, 107–118.
- Kabsch, W. (2010). *Acta Cryst.* **D66**, 125–132.
- Labasque, M., Devaux, J. J., Lévêque, C. & Faivre-Sarrailh, C. (2011). *J. Biol. Chem.* **286**, 42426–42434.
- Lonigro, A. & Devaux, J. J. (2009). *Brain*, **132**, 260–273.
- Luna-Vargas, M. P., Christodoulou, E., Alfieri, A., van Dijk, W. J., Stadnik, M., Hibbert, R. G., Sahtoe, D. D., Clerici, M., Marco, V. D., Littler, D., Celie, P. H., Sixma, T. K. & Perrakis, A. (2011). *J. Struct. Biol.* **175**, 113–119.
- Maertens, B., Hopkins, D., Franzke, C. W., Keene, D. R., Bruckner-Tuderman, L., Greenspan, D. S. & Koch, M. (2007). *J. Biol. Chem.* **282**, 10647–10659.
- Matthews, B. W. (1968). *J. Mol. Biol.* **33**, 491–497.
- Tomarev, S. I. & Nakaya, N. (2009). *Mol. Neurobiol.* **40**, 122–138.
- Waxman, S. G. & Ritchie, J. M. (1993). *Ann. Neurol.* **33**, 121–136.